Biosensors and Bioelectronics 126 (2019) 82–87

Contents lists available at ScienceDirect

Biosensors and Bioelectronics

journal homepage: www.elsevier.com/locate/bios

Calorimetric sandwich-type immunosensor for quantification of TNF-α

Saif Mohammad Ishraq Bari[a], Louis G. Reis[b], Gergana G. Nestorova[c,*]

[a] Micro and Nanoscale Systems Engineering, Louisiana Tech University, Ruston, USA
[b] Mechanical Engineering, Louisiana Tech University, Ruston, USA
[c] School of Biological Sciences, Louisiana Tech University, 1 Adams Blvd., P. O. Box 3179, Ruston, USA

ARTICLE INFO

Keywords:
Lab-on-a-chip
Calorimetric immunoassay
Microfluidics
Tumor necrosis factor-α
Thermopile

ABSTRACT

We report a lab-on-a-chip immunosesnor for quantification of the inflammatory cytokine TNF-α with picomolar sensitivity. The feasibility of the technology was demonstrated via accurate measurement of the concentration of TNF-α in astrocytes cell culture media. The immunoassay was performed in a microfluidic device with an integrated antimony/bismuth thermopile sensor and had a limit of detection of 14 pg mL^{-1}. The device was fabricated using rapid prototyping xurography technique and consisted of two inlets and single outlet. Anti-TNF-α monoclonal antibody was used to capture the analyte while the detection was performed using glucose oxidase-conjugated secondary antibody. Glucose (55 mM) was injected through a sample loop into the fluid flowing within the microfluidic device. A nanovolt meter connected to the thermoelectric sensor recorded the voltage change caused by the enzymatic reaction. Computer simulations using COMSOL Multiphysics were performed to analyze the effect of fluid velocity on the concentration of glucose within the reaction zone. A standard calibration curve was created using serial dilutions of synthetic TNF-α (0–2000 pg mL^{-1}) by plotting the area under the curve of the signal versus the concentration of the analyte. The efficacy of the device was evaluated by quantifying TNF-α in the cell culture medium of lipopolysaccharide stimulated and non-stimulated astrocytes. The results demonstrated high accuracy of the calorimetric immunoassay when compared with gold standard commercial ELISA microplate reader. The immunosensor offers excellent reproducibility, accuracy, and versatility in the choice of the detection enzyme.

1. Introduction

Tumor necrosis factor-α (TNF-α) is a biomarker that is implicated in wide range of pathological conditions and its serum concentration is commonly assayed for research and diagnostics purposes (de Gonzalo-Calvo et al., 2010). Increased level of TNF-α is associated with different pathological conditions including Alzheimer's disease (Swardfager et al., 2010), cancer (Reid et al., 1996) and inflammatory response (Arvin et al., 1996). Considering the clinical importance of TNF-α, its accurate and sensitive quantification in biological fluids is important for disease monitoring, diagnostics, and drug development. TNF-α is commonly measured using conventional immunoassays. However, tests performed in microtiter plates are time-consuming, suffer from intra and inter-assay variations and require multiple wash steps that are difficult to adapt in high-throughput setting. The sophisticated, expensive and bulky equipment and large sample volumes that are required per assay renders traditional enzyme-linked immunosorbent technology unreliable for time-sensitive measurement of TNF-α in clinical settings (Ng et al., 2010). A number of biosensors for detection of TNF-*α*have been developed that provide increased sensitivity, reduced sample volume and decreased cost per sample. Optical detection, such as florescence microscopy, has been employed for rapid quantification of TNF-α (45 pg mL^{-1}) in serum (Herrmann et al., 2008) and in cell culture medium (20 pg mL^{-1}) (Cesaro-Tadic et al., 2004). TNF-α was quantified using electrochemical immunosensing in human saliva (3.1 pg mL^{-1}) (Bellagambi et al., 2017), human serum (10 pg mL^{-1}) (Yin et al., 2011) and electrochemical impedance spectroscopy (1 pg mL^{-1}) in non-diluted human serum samples (Kongsuphol et al., 2014).

Recent years have witnessed significant progress in the development of more efficient detection technologies for lab-on-a-chip immunoassays that provide increased sensitivity and specificity for point-of-care application. Microfluidics immunosensors offer multiple advantages that include increased reaction rate, decreased time for incubation of the reactants and reduced reagents and samples consumption. Miniaturization and integration of the multiple assay components allows automation, precise control of the fluid velocity, increased reproducibility, and possibility for high-throughput analysis (Bange et al., 2005). A wide range of detection technologies has been integrated with

* Corresponding author.
E-mail address: ggnestor@latech.edu (G.G. Nestorova).

https://doi.org/10.1016/j.bios.2018.10.028
Received 31 May 2018; Received in revised form 21 August 2018; Accepted 14 October 2018
Available online 22 October 2018
0956-5663/

lab-on-a-chip biosensors for quantification of analytes in biological and chemical samples. The optimal detection method provides high sensitivity coupled with low power consumption, simple fabrication and minimal sample preparation (Pires et al., 2014). Fluorescence, chemiluminescence and electrochemiluminescnece techniques provide detection sensitivities in the ng-pg mL^{-1} range (Mohammed and Desmulliez, 2011). Reported limits of detection in fluorescence immunosensors include 0.7 ng mL^{-1} for troponin T (Mayilo et al., 2009), 0.1 pg mL^{-1} for prostate-specific antigen (PSA) (Zhu et al., 2014) and 0.05 ng mL^{-1} for okadaic acid (Pan et al., 2017). Electrochemical immunosensors offer superior sensitivity and versatility in the choice of substrate. High-sensitive detection of PSA was achieved at 3.3 fg mL^{-1} (Li et al., 2017) and the reported limit of detection for alpha-fetoprotein was 2 pg mL^{-1} (Xiong et al., 2012). Paper-based immunoassays provide fast and cost effective techniques for detection and quantification of molecular species. Some of the applications of paper-based immunoassays include HIV (Cheng et al., 2010) and influenza virus detection (Lei et al., 2015). While these detection methods are well-established, each of these techniques has limitations. Major drawbacks of the electrochemical detection technology are the effect of external factors such as pH, temperature, and ionic concentration on the performance of the assay (Sassa et al., 2008). Disadvantages of fluorescent immunosensors are the requirement for high efficiency optical filters and detectors that presents an engineering challenge in the miniaturization of the excitation and detection apparatus without significantly compromising detection sensitivity (Wu et al., 2007). Although paper-based microfluidics offers enormous potential for point-of-care devices, the overall sensitivity of the device needs to be improved (Liana et al., 2012).

While current lab-on-a-chip detection methods for TNF-α offer sensitivity, they generally require sophisticated and bulky detection systems that cannot be readily incorporated into an integrated total analysis system. Calorimetric microfluidic systems with an integrated miniaturized thermopile sensors are employed to measure small quantities of heat for biosensing applications. Since most bio-chemical reactions are accompanied by a change of heat, microfluidic calorimetry is employed in wide range of applications. This detection method is universal and allows the measurements of reactions that are not compatible with other detection methods (Lee et al., 2012). Thermopile sensors were used to monitor the metabolic rate of bacteria (Higuera-Guisset et al., 2005), cell culture for toxicity assessment (Nestorova et al., 2015), DNA sequencing (Nestorova and Guilbeau, 2011), detection of enthalpy change caused by enzymatic reactions (Tangutooru et al., 2012), quantification of DNA damage (Nestorova et al., 2015) and assessment of binding affinity (Ahmad et al., 2010).

Here we report a calorimetric sandwich-type microfluidic immunoassay for detection and quantification of TNF-α using a thin-film thermopile that is attached to the lower channel wall of the device. The calorimetric immunosensor was fabricated using xurography, an inexpensive, rapid prototyping method for the manufacture of high aspect ratio microfluidic devices. Compared to other emerging low-cost benchtop technologies like 3D printers or laser cutters, “razor writing” of thin films is as an attractive alternative for fabrication of point-of-care devices. The described method uses a cutting plotter to create microstructures from adhesive tape in less than 3 min without photolithographic processes or chemicals. Simplicity and low cost of device fabrication that does not require special facilities such as clean rooms or specialized laboratory equipment for photolithographic processing of materials are advantages derived from this manufacturing technology. The sensor converts the temperature difference caused by the enzymatic reaction between glucose and glucose oxidase conjugated TNF-α detection antibody into an electric signal that is recorded by a nanovolt meter. The total amount of heat that is generated is proportional to the concentration of analyte. The sensor is small in size (8 mm × 8 mm), light in weight, consists of 60 antimony /bismuth (Sb/Bi) thermocouple junctions and is relatively simple to fabricate. The miniaturized thermopile offers rapid response time and provides self-generating signal that does not require external power. The sensor operates without any control of external temperature because of its high common-mode thermal noise rejection ratio. The major advantages of the calorimetric immunosensor are elimination of the control of light and signal development timing, a common requirement for conventional microplate based TNF-α assays. Since calorimetric measurements are based on detection of the heat released during an enzymatic reaction, the immunoassay can be performed with wide range of enzyme-conjugated detection antibodies. The assay is performed in a flow-through system and unbound antibodies are washed away by the fluid in the microchannel. The design of the system allows the substrate to be introduced multiple times after the signal returns to baseline level to increase the statistical significance of the results. The calorimetric technique can be used for the analysis of any kind of reaction that generates measurable amount of heat. The microfluidic device requires less sample volume, the method does not need any complex sample preparation and fabrication of expendable chips can result in reduced cross-contamination. Microfluidic calorimetry offers detection of label-free biochemical components by immobilizing the enzyme, DNA or antibodies within a reaction area (Nestorova and Guilbeau, 2011; Nestorova et al., 2015).

2. Methods

2.1. Principle of calorimetric immunosensing

Calorimetric quantification of TNF-α was successfully demonstrated in a microfluidic device with an integrated thin-film Sb/Bi thermoelectric sensor with a theoretical Seebeck coefficient of 7.14 μV mK^{-1}. The technique is based on sandwiched immunodetection using a pair of matched antibodies that recognize different epitope sites of the TNF-α cytokine. The antibody/analyte complex was immobilized within the measuring junctions of the thermoelectric sensor. Fixed concentration of glucose (55 mM) was injected through a sample loop into the fluid flowing within the microfluidic device. The oxidation of glucose to gluconic acid by glucose oxidase generates 79 kJ mol^{-1} of energy (Weibel and Bright, 1971).

$$\text{Glucose} + O_2 + H_2O \xrightarrow[\text{Glucose Oxidase}]{} \text{Gluconic acid} + H_2O_2 + 79\frac{kJ}{mol}$$

The enzymatic reaction increases the localized temperature at the measuring junctions of the thermopile in respect to the reference junctions and is proportional to the concentration of TNF-α that is measured in cell culture medium of human astrocytes (Fig. 1).

2.2. Experimental set-up

A schematic of the calorimetric system for immunosensing is shown in Fig. 2. Two syringe pumps (Harvard Apparatus, Holliston, MA) independently inject sodium acetate buffer through 0.01 in. internal diameter Teflon tubing (Upchurch Scientific, Oak Harbor, WA). A sample loop that has a volume of 13 μL was loaded with 55 mM glucose that was introduced into the inlet 2 buffer stream via a 6-port injection valve (V-451, Upchurch scientific, Oak Harbor, WA). The thermal signature of the enzymatic reaction is detected and converted by the thermopile sensor to an electric signal that was measured with a nanovolt meter (Agilent, model #34430 A Loveland, CO). The output signal was recorded and processed using LabView SignalExpress software (National Instruments, Austin, TX). To prevent external electromagnetic interferences with the signal recording, the device and the nanovolt meter instrument were housed in Faraday cage.

2.3. Fabrication of immunosensor

The microfluidic device has two inlets and a single outlet for

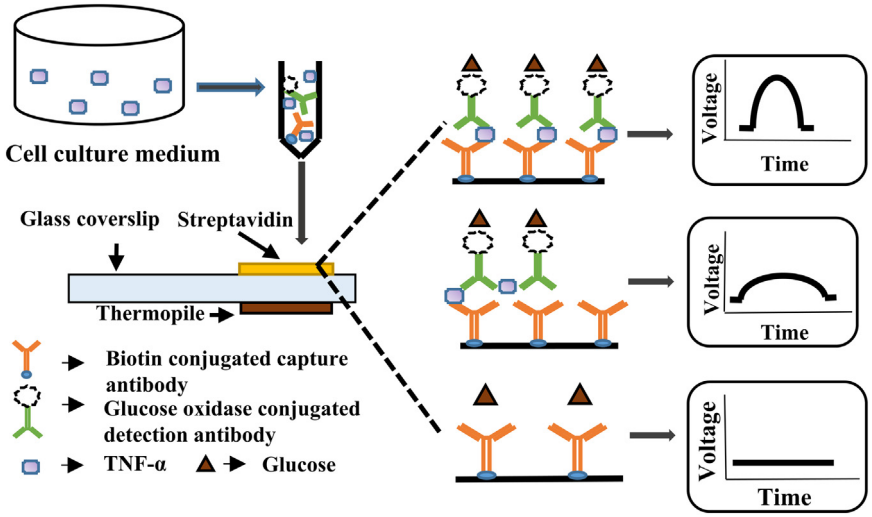

Fig. 1. Principle of calorimetric immunosensing. The amount of heat released during the enzymatic reaction between the glucose oxidase conjugated detection antibody and glucose is proportional to the concentration of TNF-α in the biological sample.

independent injection of glucose and 50 mM acetate buffer (pH 5.5) and was fabricated using rapid-prototyping technique (Fig. 3A). The channel of the device was designed using Adobe Illustrator software (Adobe, san Jose, CA) and was cut out of 100 μm thick Kapton® tape using cutting plotter (Graphtec America Inc, Santa Ana, CA). The dimensions of the channel were 65 mm × 12 mm × 0.1 mm. The upper and lower channel walls consisted of 75 mm × 25 mm × 1 mm microscope glass slide (VWR, Radnor, PA) and 75 mm × 25 mm × 0.17 mm glass cover slip (Electron Microscopy Sciences, Hatfield, PA) respectively. Streptavidin was immobilized to the lower channel wall of the device via layer-by-layer self-assembly technique. The glass coverslip was cleaned with 2% Micro 90 cleaning solution (Sigma Aldrich, St. Louis, MO). Five layers of alternating polyethylenimine (50% w/v) and polyacrylic acid (35% w/v) (Sigma Aldrich, St. Louis, MO) were applied to a carboxylated layer of the surface of the device. EZ-Link™ NHS-PEG4 Biotinylation Kit (ThermoFisher Scientific, Waltham, MA) was used to functionalize the surface with streptavidin. The sensor (Fig. 3B) was fabricated on 100 μm polyimide tape using a Denton model DV-502B metal evaporation system (Denton Vacuum, Moorestown, NJ) (Nestorova and Guilbeau, 2011) and was attached to the outer surface of the lower channel wall with silver thermal compound (Arctic Silver Inc., Visalia, CA).

2.4. Calorimetric immunoassay procedure

Human TNF-α matched antibody pair kit (ab213467, Abcam, MA) was used for the quantification of the analyte. The capture antibody was conjugated to biotin while the detection antibody was labeled with glucose oxidase using a glucose oxidase conjugation kit (ab102887, Abcam, MA) according to the vendor guidelines. Cell culture supernatant from liposaccharide (LPS) treated and non-treated human astrocytes (ScienCell Research Laboratory, Carlsbad, CA) was collected, centrifuged at 2000*g* for 10 min to remove cell debris and stored at −20 °C. A standard calibration curve was created using serial dilutions of synthetic TNF-α (0–2000 pg mL^{-1}). 20 μL of biotin linked capture antibody (2 μg mL^{-1}) and glucose oxidase conjugated detection antibody (0.5 μg mL^{-1}) were mixed with 20 μL of synthetic TNF-α and incubated on an orbital shaker for 1 h at medium speed. The same protocol was followed for the analysis of biological samples from cell culture supernatant from human astrocytes. The complex of the antibodies and the analyte was immobilized to the lower channel wall of the device via the biotin-streptavidin covalent bond. The dimensions of the reaction zone were 8 mm × 3 mm and was located directly above the measuring junctions of the sensor. Sodium acetate buffer was introduced through inlets 1 and 2 of the microfluidic device with a flow rate of 100 μL min^{-1} and 25 μL min^{-1} respectively. Glucose (55 mM) was loaded into a 13 μL sample loop and injected into the buffer stream of inlet 2 via an injection valve. The heat generated by the enzymatic reaction between the glucose and the glucose oxidase conjugated detection antibody increased the temperature at the measuring junctions of the thermopile. The magnitude of the voltage signal was calculated by integrating the area under the curve (AUC) versus time profile using

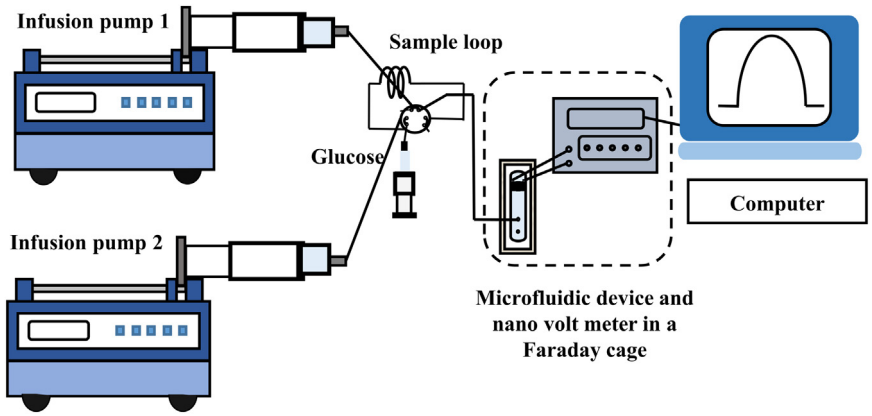

Fig. 2. Schematic diagram of the set up for calorimetric immunosensing of TNF-α.

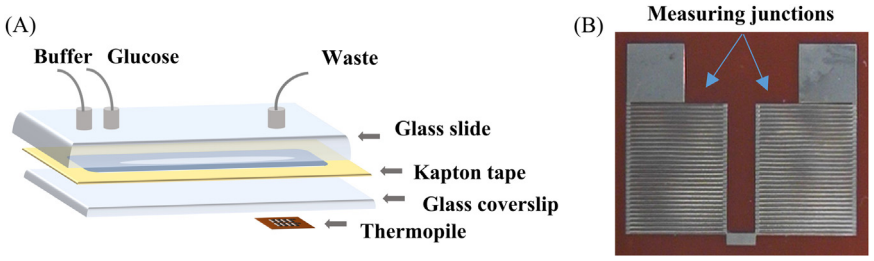

Fig. 3. (A) Microfluidic device for calorimetric detection of TNF-α. (B) Image of thin-film Sb/Bi thermopile sensor. The reaction zone was located above the measuring junctions.

the Riemann Sums trapezoid rule. Standard calibration curve was generated by plotting the concentration of synthetic TNF-α versus the average AUC of the thermoelectric response. To evaluate the accuracy of the developed immunosensor, the concentration of cytokine in cell culture supernatant was measured using human TNF-α ELISA kits (ab46087, Abcam, MA) according to the vendor's guidelines.

2.5. COMSOL simulations

The concentration of glucose along the width of the microchannel was modeled as a function of inlet 1 and inlet 2 fluid velocity. The simulations were performed using COMSOL Multiphysics 5.2a software. The developed two-dimensional stationary model was based on a microchannel with dimensions 65 mm × 12 mm. The simulation results were obtained using the laminar reacting flow module coupled with transport of diluted species module. The velocity distribution along the microchannel was assumed to follow Newtonian laminar flow. The fluid was considered as incompressible with no slip boundary conditions applied at all the walls. In order to run the simulation, physics controlled mesh with finer element size was chosen. The dimensions of the microchannel and the fluid velocity parameters used in the simulations are listed in Table 1. The velocity of inlet 1 was constant while the velocity of inlet 2 was decreased to investigate its effect on glucose distribution profile.

3. Results and discussion

3.1. COMSOL simulations of glucose concentration profile

COMSOL model has been used to characterize the distribution of the substrate along the width of the microchannel as function of inlet 2 fluid velocity. The concentration of glucose within the reaction zone was proportional to the volumetric flow rate of inlet 2 and the ratio of the fluid velocities between both inlets (Fig. 4). The buffer supplied through inlet 2 was hydrodynamically focused within the measuring junctions of the thermopile by the fluid introduced through inlet 1. Change in the velocity ratio between both inlets affected the width of the glucose stream above the reaction zone. Increase in inlet 2 velocity resulted in a wider concentration profile of the substrate (Fig. 4A and B). As a result, glucose was not confined within the measuring junctions of the thermopile which leads to an increase in the amount of heat that dissipates to the reference junctions of the sensor. Heating of the reference junctions leads to decrease in the temperature difference and reduced voltage output of the sensor. The optimal flow rates ratio of 1:4 (Fig. 4C and D) ensures that the substrate was focused within the reaction zone and minimized the heat dissipation towards the reference junctions of the sensor. In the experiments, the concentration of glucose was in excess and is not a limiting factor for the enzymatic reaction.

Table 1
Microfluidics dimensions and fluid flow model parameters.

Channel length	65 mm
Chanel width	12 mm
Internal diameter of inlet and outlet	0.254 mm (0.01 in.)
Glucose diffusion coefficient	6.7×10^{-10} m^2s^{-1} (Hannoun and Stephanopoulos, 1986)
Inlet 1 fluid velocity	6.7×10^{-4} ms^{-1}
Flow ratio	1,2, 4
Inlet 2 glucose velocity	6.7×10^{-4} ms^{-1}/Flow ratio
Reaction rate	3×10^{-7} $mol\,m^{-3}\,s^{-1}$ (Tao et al., 2009)
Inlet temperature	293.15 K
Outlet Pressure	0 atm

3.2. Standard calibration curve

Synthetic TNF-α (0 pg mL^{-1}, 125 pg mL^{-1}, 250 pg mL^{-1}, 1000 pg mL^{-1} and 2000 pg mL^{-1}) was serially diluted and incubated with the anti-TNF-α capture and glucose-oxidase conjugated detection antibodies to generate the standard calibration curve. Glucose was injected four times and the average area under the curve (AUC) of the voltage signal was calculated for each TNF-α concentration (S1). The correlation coefficient (R) was estimated to be 0.9942 that indicates an excellent correlation between the response of the microfluidic calorimetric immunosensor and the concentration of the analyte (Fig. 5A). The thermopile voltage increased as the concentration of the cytokine increased. The thermoelectric response showed a linear relationship with the TNF-α concentration in the range of 0–2000 pg mL^{-1}. The thermopile response for various concentrations of TNF-α is shown in Fig. 5B. A low level signal was measured in the negative control experiments. It is hypothesized that the thermopile responds to small temperature changes caused by the friction between the buffers supplied by the inlets of the device. The limit of detection (LOD) and limit of quantification (LOQ) of the calorimetric immunosensor were estimated from the slope of the calibration curve (0.0315) and the standard deviation of the blank (0.133) according to the following equations:

$$LOD = 3.3*\sigma/S \quad LOQ = 10*\sigma/S,$$

where σ is the standard deviation of the blank response and S is the slope of the calibration curve. The LOD of the calorimetric immunosensor was 14 pg mL^{-1} and the LOQ was 42 pg mL^{-1}. The detection and quantification limits of the fabricated microfluidic immunosensor are close to the values reported for the commercial absorbance-based ELISA kit of 10 pg mL^{-1} and 30 pg mL^{-1} respectively. The fabricated calorimetric microfluidic immunsensor has a lower LOD than those of previously reported fluorescent microfluidic sensors for quantification of TNF-α in serum (45 pg mL^{-1}) (Herrmann et al., 2008) and in cell culture medium (20 pg mL^{-1}) (Cesaro-Tadic et al., 2004).

3.3. Stability and reproducibility studies

The storage stability of the calorimetric biosensor was evaluated over a period of two weeks after storage at 4 °C. The response to glucose (55 mM) showed no changes in the average enzymatic activity at the end of the testing period (Fig. 6A).

Reproducibility analysis of within- and between assay variation was

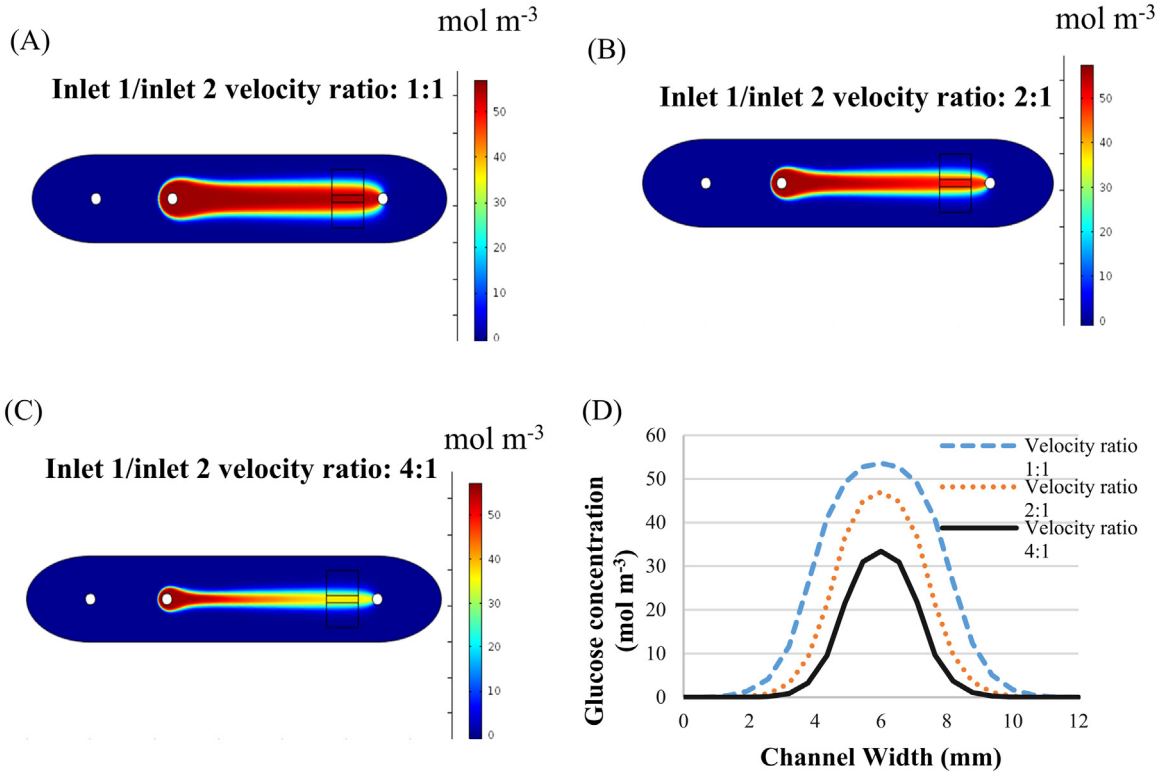

Fig. 4. Glucose concentration profile along the width of the microchannel. Inlet 1 velocity is 6.7×10^{-4} m s^{-1}. Inlet 2 flow velocity is: (A) 6.7×10^{-4} m s^{-1}; (B) 1.67×10^{-4} m s^{-1}; (C) 0.84×10^{-4} m s^{-1}. (D) Graphical representation of glucose concentration along the width of the microchannel for various flow rates of inlet 2 when the flow rate of inlet 1 was constant.

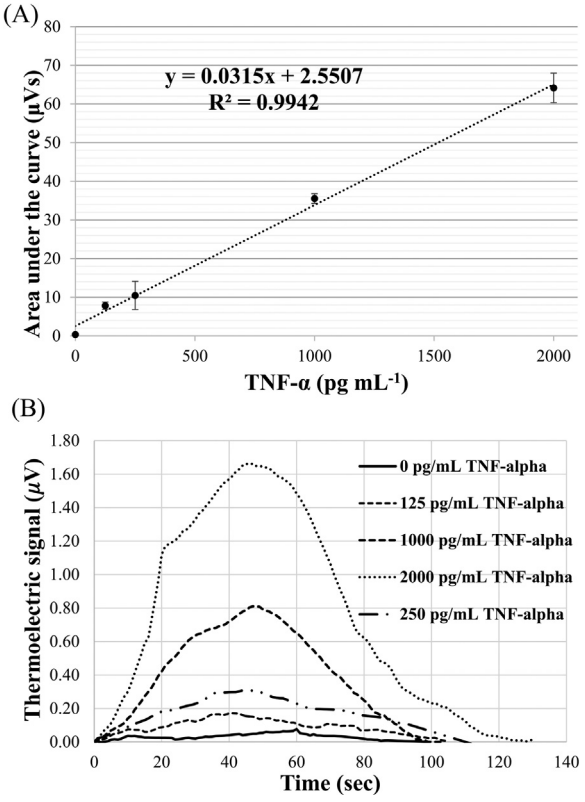

Fig. 5. (A) Standard calibration curve for calorimetric microfluidic immunosensor. (B) Thermopile voltage output for various concentrations of synthetic TNF-α.

performed using three immunosensing devices (250 pg mL^{-1} TNF-α). The co-efficient of variation between assays was 0.99%. The intra-assay coefficient of variation for three different devices were 0.72%, 0.24% and 0.47% respectively, see S2. Potential sources that add to the assay variation include minor differences in the Seebeck coefficient of the thermoelectric sensor, the position of the antibody/analyte complex within the junctions of the thermopile, as well as variations of the enzyme labeling efficiency of the detection antibody. The friction of the two buffer streams supplied at different velocity generates low levels of non-specific heat that can be detected by the sensor.

3.4. TNF-α concentration in cell culture medium

The feasibility of applying the sensor for analysis of biological samples was investigated via quantification of TNF-α in cell culture media samples and comparison of the levels measured using the microfluidic immunosensor and conventional ELISA. The equation of standard calibration curve was used to calculate the concentration of TNF-α in the cell culture medium of non-treated and lipopolysaccharide (100 ng mL^{-1}) treated human astrocytes using the calorimetric technique. The levels of the cytokine in the biological samples were measured using a conventional ELISA kit and the results were compared to assess the accuracy of the microfluidic platform (Fig. 6B).

The concentration of TNF-α in lipopolysaccharide treated cells was 252 pg mL^{-1} and 251 pg mL^{-1} for absorbance based ELISA and the calorimetric immunosensor respectively. The levels of TNF-α in non-treated astrocytes measured using conventional ELISA (170 pg mL^{-1}) and the microfluidic device (169 pg mL^{-1}) have less than 1% variation. The developed biosensor exhibited good selectivity as TNF-α determinations agreed well with the standard immunoassay analysis. The microfluidic immunosensor had lower inter assay variability in comparison to absorbance based microplate immunoassay. There was no significant difference between the results obtained by the two methods

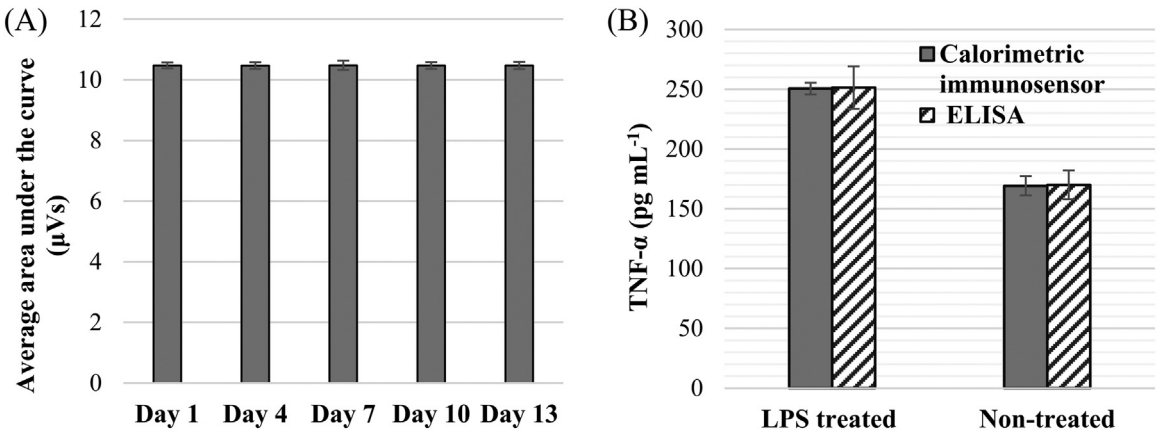

Fig. 6. (A) Stability study after storage at 4 °C. (B) Concentration of TNF-*α* in the cell culture medium of lipopolysaccharide treated and non-treated human astrocytes measured using conventional micro plate based ELISA and calorimetric immunosensor (n = 4).

and therefore the proposed immunosenor can be reasonably applied for analysis of biological samples.

4. Conclusion

This paper describes the design and fabrication a microfluidic immunosensor with an integrated thin-film thermopile for quantification of TNF-α in biological samples. The developed calorimetric device can detect low levels of heat and utilizes a glucose oxidase conjugated antibody as a novel method for sensitive detection of TNF-α. The assay is based on a sandwich-type immunodetection where the enzymatic reaction between the substrate and the enzyme generates heat that is converted to an electrical signal by the thermoelectric sensor. The calorimetric immunosensor had a low limit of detection of 14 pg mL^{-1}. This novel calorimetric method for quantification of TNF-α could be easily extended for sensitive detection of various analytes in biological samples.

Acknowledgments

This work was supported by Louisiana Board of Regents RCS grant LEQSF (2018-21)-RD-A-27.

Appendix A. Supporting information

Supplementary data associated with this article can be found in the online version at doi:10.1016/j.bios.2018.10.028.

References

Ahmad, L.M., Towe, B., Wolf, A., Mertens, F., Lerchner, J., 2010. Sens. Actuators B Chem. 145, 239–245.
Arvin, B., Neville, L.F., Barone, F.C., Feuerstein, G.Z., 1996. Neurosci. Biobehav. Rev. 20, 445–452.
Bange, A., Wong, D.K.Y., Seliskar, C.J., Halsall, H.B., Heineman, W.R., 2005. Microfluid., BioMEMS, Med. Microsyst. III 5718, 142–151.
Bellagambi, F.G., Baraket, A., Longo, A., Vatteroni, M., Zine, N., Bausells, J., Fuoco, R., Di Francesco, F., Salvo, P., Karanasiou, G.S., Fotiadis, D.I., Menciassi, A., Errachid, A., 2017. Sens. Actuators B Chem. 251, 1026–1033.
Cesaro-Tadic, S., Dernick, G., Juncker, D., Buurman, G., Kropshofer, H., Michel, B., Fattinger, C., Delamarche, E., 2004. Lab Chip 4, 563–569.
Cheng, C.-M., Martinez, A.W., Gong, J., Mace, C.R., Phillips, S.T., Carrilho, E., Mirica, K.A., Whitesides, G.M., 2010. Angew. Chem. Int. Ed. 49, 4771–4774.
de Gonzalo-Calvo, D., Neitzert, K., Fernández, M., Vega-Naredo, I., Caballero, B., García-Macía, M., Suárez, F.M., Rodríguez-Colunga, M.J., Solano, J.J., Coto-Montes, A., 2010. Free Radic. Biol. Med. 49, 733–737.
Hannoun, B.J.M., Stephanopoulos, G., 1986. Biotechnol. Bioeng. 28, 829–835.
Herrmann, M., Veres, T., Tabrizian, M., 2008. Anal. Chem. 80, 5160–5167.
Higuera-Guisset, J., Rodríguez-Viejo, J., Chacón, M., Muñoz, F.J., Vigués, N., Mas, J., 2005. Thermochim. Acta 427, 187–191.
Kongsuphol, P., Ng, H.H., Pursey, J.P., Arya, S.K., Wong, C.C., Stulz, E., Park, M.K., 2014. Biosens. Bioelectron. 61, 274–279.
Lee, W., Lee, Koh, 2012. Nanobiosensors Dis. Diagn. 1, 17–29.
Lei, K.F., Huang, C.-H., Kuo, R.-L., Chang, C.-K., Chen, K.-F., Tsao, K.-C., Tsang, N.-M., 2015. Anal. Chim. Acta 883, 37–44.
Li, M., Wang, P., Li, F., Chu, Q., Li, Y., Dong, Y., 2017. Biosens. Bioelectron. 87, 752–759.
Liana, D.D., Raguse, B., Gooding, J.J., Chow, E., 2012. Sensors 12, 11505–11526.
Mayilo, S., Kloster, M.A., Wunderlich, M., Lutich, A., Klar, T.A., Nichtl, A., Kürzinger, K., Stefani, F.D., Feldmann, J., 2009. Nano Lett. 9, 4558–4563.
Mohammed, M.-I., Desmulliez, M.P.Y., 2011. Lab Chip 11, 569–595.
Nestorova, G.G., Guilbeau, E.J., 2011. Lab Chip 11, 1761–1769.
Nestorova, G.G., Kopparthy, V.L., Crews, N.D., Guilbeau, E.J., 2015. Anal. Methods 7, 2055–2063.
Ng, A.H.C., Uddayasankar, U., Wheeler, A.R., 2010. Anal. Bioanal. Chem. 397, 991–1007.
Pan, Y., Zhou, J., Su, K., Hu, N., Wang, P., 2017. Procedia Technol. 27, 214–216.
Pires, N., Dong, T., Hanke, U., Hoivik, N., 2014. Sensors 14, 15458–15479.
Reid, S.E., Murthy, M.S., Kaufman, M., Scanlon, E.F., 1996. Br. J. Surg. 83, 1037–1046.
Sassa, F., Morimoto, K., Satoh, W., Suzuki, H., 2008. Electrophoresis 29, 1787–1800.
Swardfager, W., Lanctôt, K., Rothenburg, L., Wong, A., Cappell, J., Herrmann, N., 2010. Biol. Psychiatry 68, 930–941.
Tangutooru, S.M., Kopparthy, V.L., Nestorova, G.G., Guilbeau, E.J., 2012. Sens. Actuators B Chem. 166–167, 637–641.
Tao, Z., Raffel, R.A., Souid, A.-K., Goodisman, J., 2009. Biophys. J. 96, 2977–2988.
Weibel, M.K., Bright, H.J., 1971. J. Biol. Chem. 246, 2734–2744.
Wu, J., Fu, Z., Yan, F., Ju, H., 2007. TrAC Trends Anal. Chem. 26, 679–688.
Xiong, P., Gan, N., Cao, Y., Hu, F., Li, T., Zheng, L., 2012. Materials 5, 2757–2772.
Yin, Z., Liu, Y., Jiang, L.-P., Zhu, J.-J., 2011. Biosens. Bioelectron. 26, 1890–1894.
Zhu, Y.-D., Peng, J., Jiang, L.-P., Zhu, J.-J., 2014. Analyst 139, 649–655.